pubs.acs.org/Biomac

Article

Cationic Cross-Linked Nanocellulose-Based Matrices for the Growth and Recovery of Intestinal Organoids

Rodrigo Curvello and Gil Garnier*

Cite This: *Biomacromolecules* 2021, 22, 701−709

Read Online

ACCESS | Metrics & More | Article Recommendations | Supporting Information

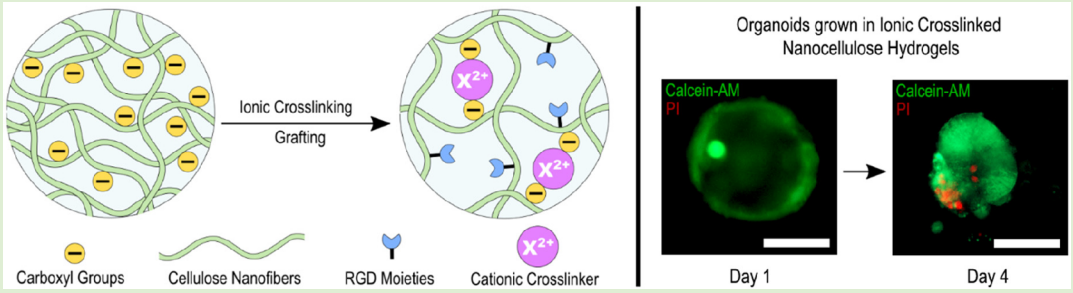

ABSTRACT: Highly carboxylated nanocellulose fibers can be functionalized with cell adhesive peptides and cationic cross-linked to form matrices for a three-dimensional (3D) cell culture. It is hypothesized that nanocellulose hydrogels cross-linked with divalent cations can provide the required biochemical and mechanical properties for intestinal organoid growth and recovery. Nanocellulose hydrogels are produced by TEMPO- and TEMPO-periodate-mediated oxidation and functionalized with RGD peptides. Mechanical properties are measured by rheology and optical properties quantified by UV−vis spectroscopy. Cellulosic matrices are cross-linked with Ca^{2+} and Mg^{2+} and intestinal organoids cultured for 4 days. The organoids are recovered for passaging and RNA extraction. TEMPO-periodate-oxidized nanocellulose fibers form functionalized hydrogels and support the growth of intestinal organoids. The highly transparent cellulosic matrix requires 4 times more Mg^{2+} than Ca^{2+} ions to reach the targeted stiffness. Organoids cultured in nanocellulose maintained a major living area for up to 4 days. Cell clusters recovered from magnesium-cross-linked hydrogels can be passaged, and their extracted RNA is intact. Cationic cross-linked nanocellulose hydrogels are promising alternative plant-based matrices for a 3D cell culture systems.

INTRODUCTION

Hydrogels are porous three-dimensional structures that hold large amounts of water while presenting some mechanical integrity.[1,2] This class of soft materials rely on a physically or chemically cross-linked network of fibers and can be responsive to changes in temperature, pH, and radiation.[3−5] Apart from synthetic polymers, many natural biopolymers have been explored for the synthesis of hydrogels, highlighting the potential of cellulose, alginate, and chitosan.[6−8] From those, cellulose is the most abundant carbohydrate polymer on Earth, present in bacteria and plants. Depending on its source, cellulose bundles can be isolated into nanofibers 2−60 nm in diameter and several micrometers in length.[9,10] The 2,2,6,6-tetramethylpiperidine-1-oxyl (TEMPO)-mediated oxidation has been commonly used to convert the primary alcohol groups (C2) of cellulose chains into negatively charged carboxylate groups.[11] Recently, Mendoza et al. introduced a one-shot TEMPO-periodate oxidation method able to achieve a higher degree of substitution by targeting the C2, C3, and C6 positions in the cellulose molecule.[12] Both TEMPO- and TEMPO-periodate-oxidized nanocellulose (TON and TPON, respectively) can be mechanically defibrillated by high-pressure homogenization to form hydrogels.[13,14] The colloidal stability of these hydrogels relies on an entangled network of nanofibers, which can be further modified by covalent or ionic cross-linking. Additives, such as amino acids and sugars, can also be dissolved in these hydrogels for designing their biochemical properties to achieve specific levels of osmolality and ionic strength.[15] Because of its great tunability, allied to its biocompatibility, plant-based nanocellulose hydrogels are ideal candidates for biomedical applications.[10] Indeed, literature reports such use of cellulosic hydrogels in a three-dimensional (3D) cell culture, tissue engineering, drug delivery, and wound dressing.[16−19]

Three-dimensional (3D) cell culture systems are robust biological models that mimic the behavior and properties of human tissues and organs by combining cells to biomaterials

Received: October 20, 2020
Revised: December 5, 2020
Published: December 17, 2020

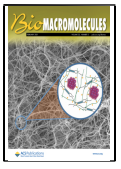

and a range of growth factors.[20−22] The cluster of cells cultured within these controlled microenvironments are named organoids or spheroids; these are commonly applied to drug testing and design as well as disease modeling.[23−25] Despite the use of scaffold-free methods, the growth of organoids and spheroids commonly relies on a poorly defined tumor-derived matrix extracted from the Engelbreth−Holm−Swarm (EHS) mouse sarcoma.[26] Commercially know as Matrigel, this animal-based matrix presents a high variability between batches and a consistency as low as 50%.[27] The limited tunability of Matrigel and its restricted range of stiffness as well as high cost represent critical limitations for *in vitro* assays in medical research.[26,28] These limitations have hindered the translation of organoids into clinics as well as limited the reproducibility of experimental assays. Therefore, fully defined matrices that match the mechanical, chemical, and biological properties of Matrigel and its counterparts are urgently needed. Over the past years, a plethora of synthetic and natural hydrogels have emerged as potential alternatives to grow a variety of organoids and spheroids.[6,29−33] Cellulose-based hydrogels have been mostly explored as a mechanical scaffold for these cultures, but with no biochemical modifications to achieve optimum cell−surface interaction. Indeed, neat cellulose gels were previously reported for the culture of tumor liver spheroids as well as for the differentiation of liver organoids.[16,34] Recently, functionalized nanocellulose hydrogels were introduced for the growth of intestinal organoids. However, the stiffness of these gels was proportional to their solids content, and the effect of multiple cross-linkers and their concentration were not assessed.[35] Last, the recovery of spheroids and organoids grown in cellulosic matrices, even for short-term passaging, has not been deeply investigated.

Here, we investigate cationic cross-linking to control the mechanical properties of nanocellulose hydrogels for the growth and recovery of intestinal organoids. We raise the hypothesis that highly carboxylated cellulosic nanofibers can form a functionalized matrix presenting the ideal biochemical and physical properties for organoid growth. TON and TPON fibers are grafted with fibronectin-derived peptides, and the effects on the hydrogel as well as on the development of organoids are assessed. The mechanical properties of TPON hydrogels cross-linked with Ca^{2+} and Mg^{2+} are characterized from a rheological perspective. Organoids are cultured in these cellulosic matrices for 4 days and recovered for passaging and RNA extraction. This study demonstrates the feasibility of cationic cross-linked nanocellulose-based hydrogels as a sustainable and promising material for 3D cell culture systems.

MATERIALS AND METHODS

Materials. Never-dried Bleached Eucalyptus Kraft (BEK) pulp was kindly supplied by Australian Paper, Maryvale, Australia. Sodium bromide (NaBr, 71329), sodium periodate ($NaIO_4$, 311448), 2,2,6,6-tetramethylpiperidine-1-oxyl (TEMPO, 214000), sodium hydroxide (NaOH, S8045), sodium chloride (NaClO, 425044), 2-(*N*-morpholino)ethanesulfonic acid (MES, M0164), glycine (50046), 1-ethyl-3-(3-(dimethylamino)propyl)carbodiimide (EDC, E6383), *N*-hydroxysuccinimide (NHS, 130672), 4-(2-hydroxyethyl)-1-piperazineethanesulfonic acid (HEPES, H7523) propidium iodade (PI, P4170), and calcein-AM (C1359) were purchased from Sigma-Aldrich. Growth Factor Reduced (GFR) Matrigel (356231) was purchased from Corning. Sodium chloride (NaCl, 1064040500) was purchased from Merk. GRGDSPC (RGD) peptides were synthesized by and purchased from GenScript. Gibco Dulbecco's Modified Eagle Medium Nutrient Mixture F-12 (DMEM/F12, 11320033), Glutamax (35050061), N2 (17502001), B27 (0080085SA), HEPES (15630080), and penicillin−streptomycin (Pen-Strep, 15140122) were purchased from Thermo Fisher Scientific. Recombinant Murine EGF (315-09) was purchased from Peprotech, RLT buffer (79216) and RNeasy Micro Ki were purchased from QIAGEN, and GelRed nucleic acid gel stain was purchased from Biotium.

Synthesis of Nanocellulose Hydrogels. Nanocellulose hydrogels were synthesized by TEMPO- and TEMPO-periodate-mediated oxidation according to Saito et al. and Mendoza et al.[11−13] Briefly, a mass of 10 g of never-dried Bleached Eucalyptus Kraft (BEK) (Australian Paper, Maryvale, Australia) pulp was disintegrated and suspended in 1200 mL of distilled water containing proportional amounts of TEMPO, NaBr, and $NaIO_4$. To avoid photoinduced decomposition, the reaction beaker was covered with aluminum foil. The oxidation was initiated by the dropwise addition of 12% w/v NaClO, pH 10.5, at a ratio of 8 mmol NaClO/g fibers. The pH was maintained at 10.5 by the addition of 0.5 M NaOH. The reaction was interrupted after 4 h by adding 10 mL of ethanol. The oxidized fibers were recovered and washed several times with distilled water through a vacuum filtration and stored refrigerated (4 °C). The conductivity of the oxidized samples was monitored throughout the titration progress, and the carboxyl group content (mmol COO^-Na^+/g fiber) was quantified as

$$\mathrm{CC} = \frac{c(V_2 - V_1)}{w} \tag{1}$$

where V_1 and V_2 are the amount of titrant (start and end of conductivity titration curve) required to neutralize the carboxylic groups (in mL), c is the NaOH concentration (mol/L), and w is the sample weight (g). The oxidized pulp was disintegrated in deionized water (0.1 and 0.3 wt % solids content) and passed twice through a high-pressure homogenizer (GEA Niro Soavi Homogenizer Panda) at 1000 bar to form hydrogels by mechanical fibrillation.

Nanocellulose Hydrogels Functionalization. TEMPO-periodate-oxidized nanocellulose fibers were grafted with RGD peptides by EDC/NHS coupling. EDC and NHS were dissolved in a MES buffer containing NaCl 0.9% at pH 6. EDC and NHS were mixed to the hydrogel in a molar ratio 1:1.5:1 to the existing carboxylate group concentration and stirred 15 min at room temperature. A volume of RGD peptides was added to the hydrogel at the final concentration of 2 mM and stirred for 2 h at room temperature. The pH of the grafted NC hydrogel was adjusted to 7 by adding NaOH (1 M) as measured by pH strips. Glycine (250 mM) and HEPES (25 mM) were dissolved in the hydrogel, and a volume of 100 μL was used to quantify the hydrogel osmolality in a K-7400S osmometer (Knauer). Hydrogels were sterilized under ultraviolet radiation exposure at a dose of 250 nm for 20 min within a Safemate ECO Class 2 Biological Safety Cabinet before in culture.

Rheology. Matrigel and nanocellulose hydrogels were characterized by rheology using an Anton Paar MCR302 rheometer with a parallel plate (PP25, ϕ = 25 mm). The viscosity and oscillatory strain sweep measurements were performed, and a solvent trap was used to ensure temperature stability. The viscosity was measured at shear rates of 0.5−100 s^{-1}. The oscillatory strain sweep was measured between 0.01 and 100% strain at constant 1 Hz frequency; this assay also measured the shear stress vs shear strain. For each replicate, a volume of 1 mL of nanocellulose hydrogels was cross-linked with 100 μL of $CaCl_2$ or $MgCl_2$ (50−200 mM) and incubated at room temperature for 5 min. Similarly, 1 mL of Matrigel was incubated at 37 °C and 5% CO_2 for 15 min. Samples were covered with organoid culture media and incubated at 37 °C for 3 h. After incubation, the culture media was removed and the hydrogels or Matrigel transferred to the rheometer surface for measurements. All measurements were performed in triplicates to ensure reproducibility.

UV−Vis Spectroscopy. A volume of 1 mL of functionalized hydrogels (RGD-TON and RGD-TPON) and Matrigel was added to plastic cuvettes. Matrigel was incubated at 37 °C for 15 min for polymerization. Air bubbles were removed by centrifugation at 4000 rpm for 5 min. The transmittance spectra between 300 and 100 nm

https://dx.doi.org/10.1021/acs.biomac.0c01510
Biomacromolecules 2021, 22, 701−709

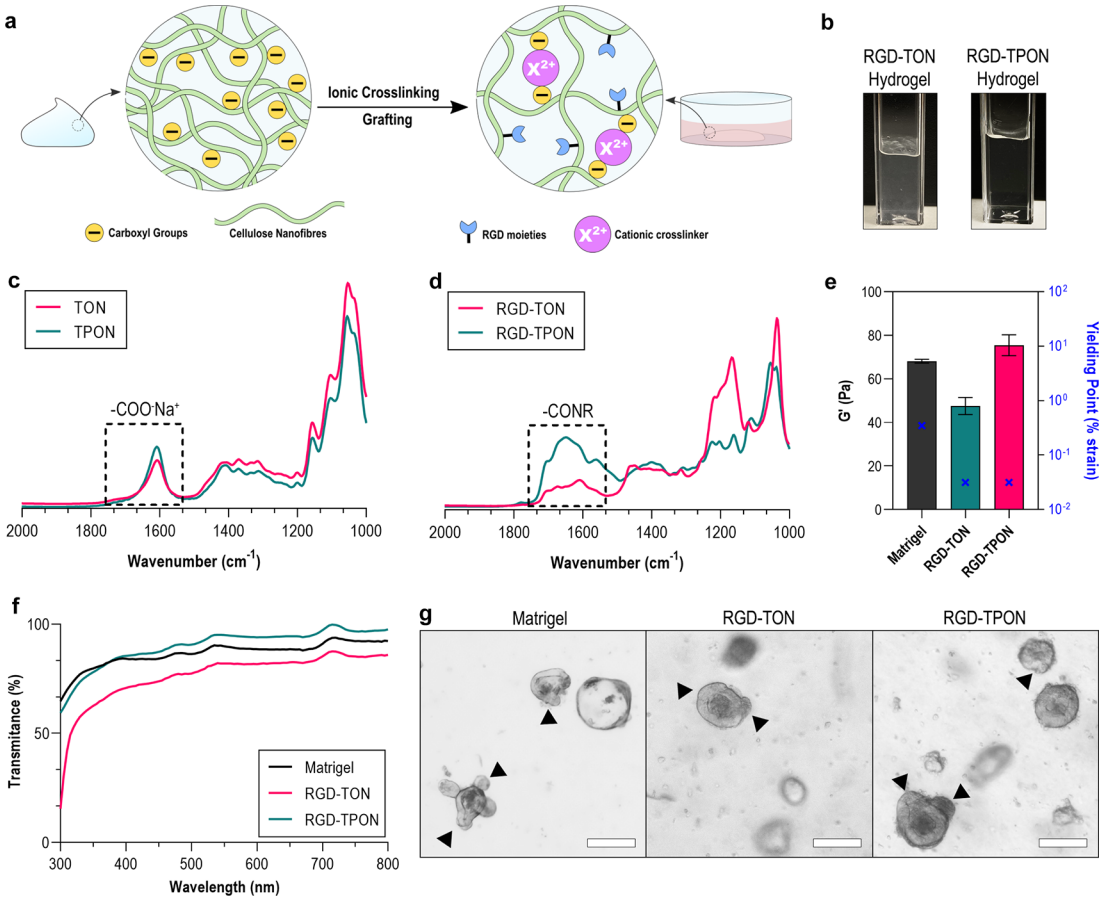

Figure 1. Ionic cross-linked nanocellulose matrices. (A) Overview of the ionic cross-linking of functionalized nanocellulose matrix. (B) RGD-TON and RGD-TPON hydrogels. HATR-FTIR spectra of (C) neat TON and TPON hydrogels and (D) RGD-TON and RGD-TPON hydrogels. (E) Storage modulus (G') and yielding point of the cellulosic matrices with comparison to Matrigel. (F) Light transmittance of the RGD-TPON hydrogel is nearly 100%, Matrigel is lower at 90%, and RGD-TON is 70%. (G) Intestinal organoids embedded in RGD-TPON hydrogel grow within 4 days of culture with prominent signals of budding, while those in RGD-TON have smaller budding regions (indicated by arrows). Scale bars: 100 μm. Results shown represent independent experiments performed in triplicates (n = 3, error bars = SD).

were measured by UV−vis spectrometry (Cary 60 UV−vis, Agilent Technologies).

Cross-Linking Density. The cross-linking density was calculated according to Flory−Rehner theory[36] as

$$n = \frac{G'}{RT} \tag{2}$$

where G' (Pa) is the storage modulus, R is the gas constant (8.314 J mol^{-1} K^{-1}), and T is the temperature (298 K).

Intestinal Organoids Establishment. All animal procedures were approved by the Monash Animal Ethics Research Platform ethics committee in strict accordance with good animal practice as defined by the National Health and Medical Research Council (Australia) Code of Practice for the Care and Use of Animals for Experimental Purposes. Briefly, mice (*Mus musculus*) were culled by cervical dislocation. The small intestine tube was dissected and flushed with PBS to remove faeces. Small intestinal tissues were opened longitudinally and scraped with a glass coverslip to remove villi. Samples were cut into 5 mm pieces and washed five times with PBS to remove unattached epithelial fragments, mucus, and residual faeces. After incubation for 30 min at 4 °C in 3 mM EDTA-PBS solution, intestinal crypts were released from the small intestine tissue fragments by mechanically pipetting up and down with a 10 mL pipet in PBS. Isolated intestinal crypts were strained (70 μm cell strainer, Falcon) and pelleted by centrifugation three times at 1500 rpm for 2 min at 4 °C. The crypts were resuspended in Growth Factor Reduced (GFR) Matrigel for organoid establishment. A volume of Matrigel and isolated crypts (50 μL) was seeded into each well of a 24-well plate (Nunc) and incubated for 15 min at 37 °C until solidified. Each well received 500 μL of crypt culture media (DMEM/F12, 10% R-spondin 1 conditioned media, 2% Noggin conditioned media, 0.5 μg/mL Amphotericin B, Glutamax, N2, B27, 10 mM HEPES, Pen-Strep, 50 ng/mL EGF). Crypt culture media was replaced every 2 days.

Organoid Culture and Passaging. Once established, intestinal organoids were passaged every 3 days. For passaging, Matrigel was mechanically disrupted and the organoids were recovered by centrifugation (3 min at 1500 rpm). Residual volumes of Matrigel were removed, and organoids were resuspended in DMEM/F12 media followed by mechanical disruption or dissociation achieved by manual pipetting for at least 30 times. Intestinal crypts were washed with 5 mL of DMEM/F12 media for 3 min at 1500 rpm and resuspended in Matrigel or nanocellulose hydrogels. A volume of 50 μL of Matrigel-containing crypts was seeded into a 24-well plate as previously described. For nanocellulose, a 24-well plate was first coated with 5 μL of $CaCl_2$ or $MgCl_2$ solution and then followed by the seeding of 50 μL of hydrogels containing intestinal crypts. Hydrogels were incubated for 5 min at room temperature. Each well, containing crypts embedded in Matrigel or ionic cross-linked hydrogels, received 500 μL of crypt culture media, replaced every 2 days. The same protocol was repeated for the further passages of organoids in Matrigel or hydrogels.

Viability Test and Colony Forming Efficiency. Small intestinal organoids embedded in the nanocellulose hydrogels or Matrigel were cultured for 2 or 4 days and stained with propidium iodide and Calcein-AM to assess living and dead areas. The crypt culture media was replaced by 500 μL of DMEM/F12 media containing 3 μM mM

https://dx.doi.org/10.1021/acs.biomac.0c01510
Biomacromolecules 2021, 22, 701−709

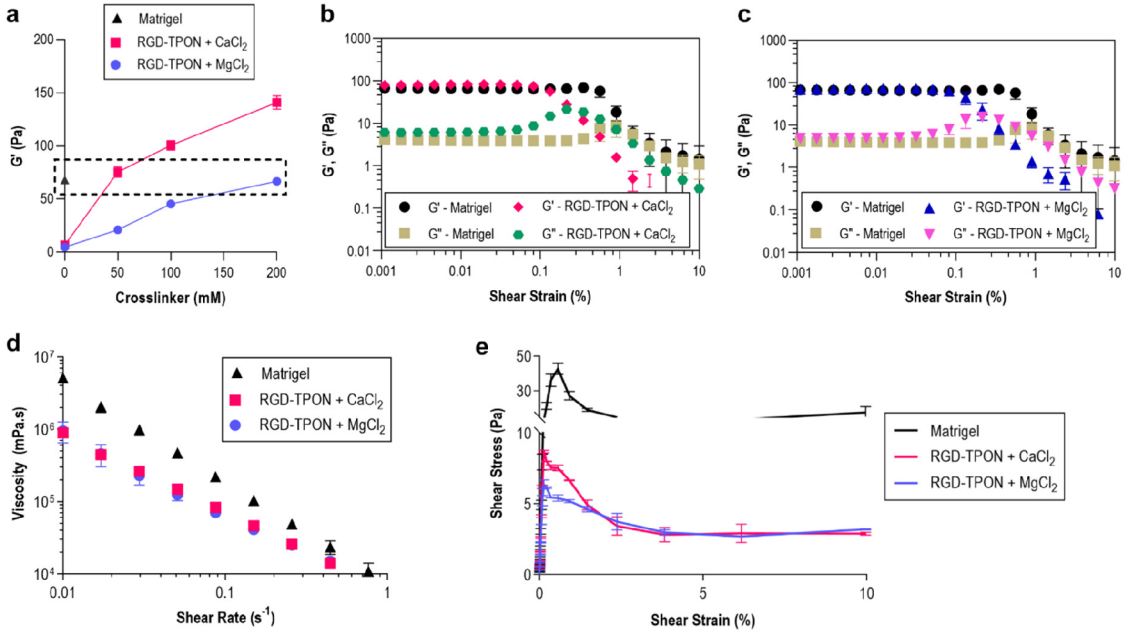

Figure 2. Rheological characterization of cationic cross-linked hydrogels. (A) Nanocellulose hydrogels require 4 times more Mg^{2+} than Ca^{2+} ions to reach the stiffness of Matrigel. Storage and loss moduli of RGD-TPON cross-linked with (B) $CaCl_2$ and (C) $MgCl_2$ are similar to Matrigel. (D) In spite of the cationic cross-linker, RGD-TPON hydrogels retain a shear-thinning behavior. (E) Mg^{2+}-cross-linked matrix yields under 6 Pa, while those containing Ca^{2+} flow under 9 Pa. Results shown represent independent experiments performed in triplicates (n = 3, error bars = SD).

propidium iodide and 1 μM Calcein-AM. Organoids were incubated at 37 °C and 5% CO_2 for 30 min protected of light. Organoids were imaged under an EVOS XL Core microscope. The numbers of organoids within both matrices were manually quantified by ImageJ and data processed.

RNA Extraction. Matrigel and nanocellulose hydrogels were mechanically disrupted with a pipet to dislodge the organoids. Organoids were recovered by centrifugation (3 min at 1500 rpm), and the residual volumes of Matrigel and hydrogels were removed. RNA was extracted by using a RNeasy Micro Kit according to the manufacturer's instructions. Briefly, organoids were resuspended in RLT buffer and incubated at room temperature for 5 min. The proportional volume of 70% ethanol was added, and samples were transferred to a Qiagen RNeasy microcolumn. Samples were centrifuged at 8000g for 15 s and treated with RW1 and DNase and RPE solutions. Samples were recovered in RNase-free water, and the preliminary quantification was assessed by a Nanodrop 2000 (ThermoFisher Scientific). To validate the integrity of RNA, samples were separated by agarose gel electrophoresis and evaluated through a bioanalyzer. A 2% gel was prepared by using agarose powder dissolved in 1× TAE buffer (40 mM Tris-Base, 20 mM glacial acetic acid, 1 mM EDTA). After cooling slightly, GelRed (1 μL per 100 mL of gel) was added, and agarose was poured into a casting tray. A 5× loading dye (50% glycerol, 50% Milli-Q water, and 0.01% Orange G dye powder) was added to samples before loading. Electrophoresis was performed at 85 V for 40 min. The gel was imaged under a Bio-Rad Gel Doc Unit (Bio-Rad). RNA samples were sent to Monash Health Translation Precinct—Medical Genomics Facility to be assessed through an Agilent bioanalyzer.

Statistical Analysis. The statistically significant differences in the colony forming units were assessed by unpaired t test with Welch's correction in GraphPad Prism 8.

RESULTS

Grafting RGD Peptides on Nanocellulose Fibers. The carboxyl group contents of TON and TPON were quantified as 0.98 and 1.92 mmol COO^-/g fiber (Figure S1), and the chemical structure of neat and functionalized nanocellulose fibers was characterized by FTIR spectroscopy. The spectra of oxidized nanocellulose reveal the characteristics OH and CH stretching at 3300 and 2900 cm^{-1}, respectively. The carboxylate groups are detected by the peak at 1615 cm^{-1} with higher intensity for TPON than for TON (Figure 1c). Grafted oxidized nanocellulose presents peaks between 1630 and 1690 cm^{-1}, the characteristic absorption of amide C═O stretch. This shows the formation of covalent bonds between the TON and TPON fibers and the cell adhesive molecule mediated by EDC/NHS coupling (Figure 1d).

Stiffness and Optical Properties of Cellulose-Based Matrices. The storage modulus (G') of Matrigel is measured to be 66 Pa, and the nanocellulose hydrogels were designed to match their rheological properties (Figure 1e). RGD-TON and RGD-TPON hydrogels at 0.1 wt % solids content present a poor stiffness (G') and a liquidlike dominant profile, respectively, as measured by the parallel plate geometry (Figure S2). When ionic cross-linked with $CaCl_2$ (50 mM), RGD-TON hydrogels reach G' = 47 Pa while RGD-TPOF achieves 75 Pa. The cross-linking density for cross-linked RGD-TON hydrogels is quantified as 20.49 mmol/m^3, while for RGD-TPON it is 31.14 mmol/m^3 (Table S1). Hydrogels at 0.3 wt % grafted oxidized nanocellulose form significantly stiffer matrices of G' up to 500 Pa (Figure S3). RGD-TPON hydrogels are highly transparent, allowing nearly 100% of light transmission between 400 and 1000 nm. By comparison, the light transmittance of Matrigel is 90% but higher than RGD-TON hydrogels at 70% (Figure 1f).

Intestinal Organoid Growth in RGD-TON and TPON Hydrogels. The growth of intestinal organoids in Matrigel, RGD-TON, and RGD-TPON hydrogels cross-linked with $CaCl_2$ (50 mM) was followed by optical microscopy. After 4 days of culture, organoids in all these matrices are formed and present a diameter up to 100 μm. Organoids in Matrigel have different morphologies and can present multiple budding structures (crypt-like domains that mimic the intestine), indicated by arrows. In contrast, those encapsulated in RGD-

https://dx.doi.org/10.1021/acs.biomac.0c01510
Biomacromolecules 2021, 22, 701−709

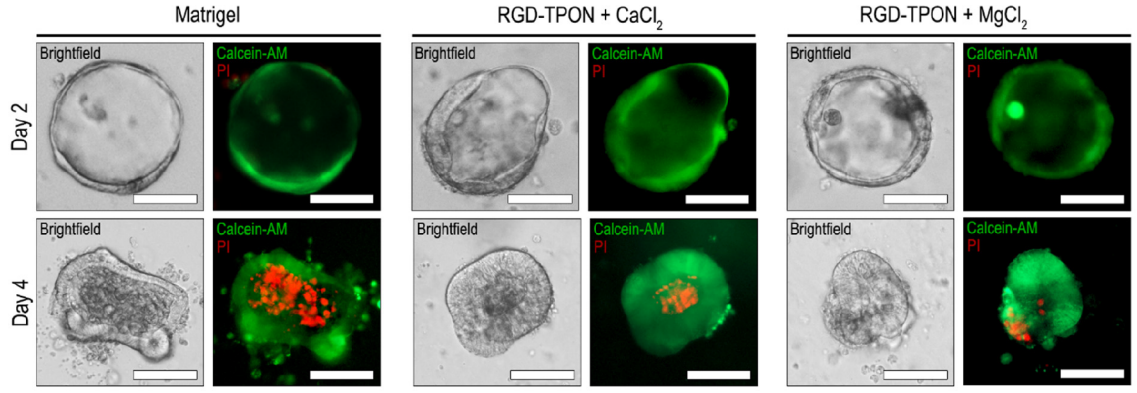

Figure 3. Intestinal organoid viability. Intestinal organoids were seeded in Matrigel and RGD-TPON hydrogels cross-linked with $CaCl_2$ and $MgCl_2$. During the second day of culture, cystic organoids present a major viable area. On the fourth day, organoids in Matrigel and RGD-TPON hydrogels show signals of budding and maintain a high viability with a minor population of apoptotic cells. Scale bars: 100 μm. Results shown represent independent experiments performed in triplicates (n = 3).

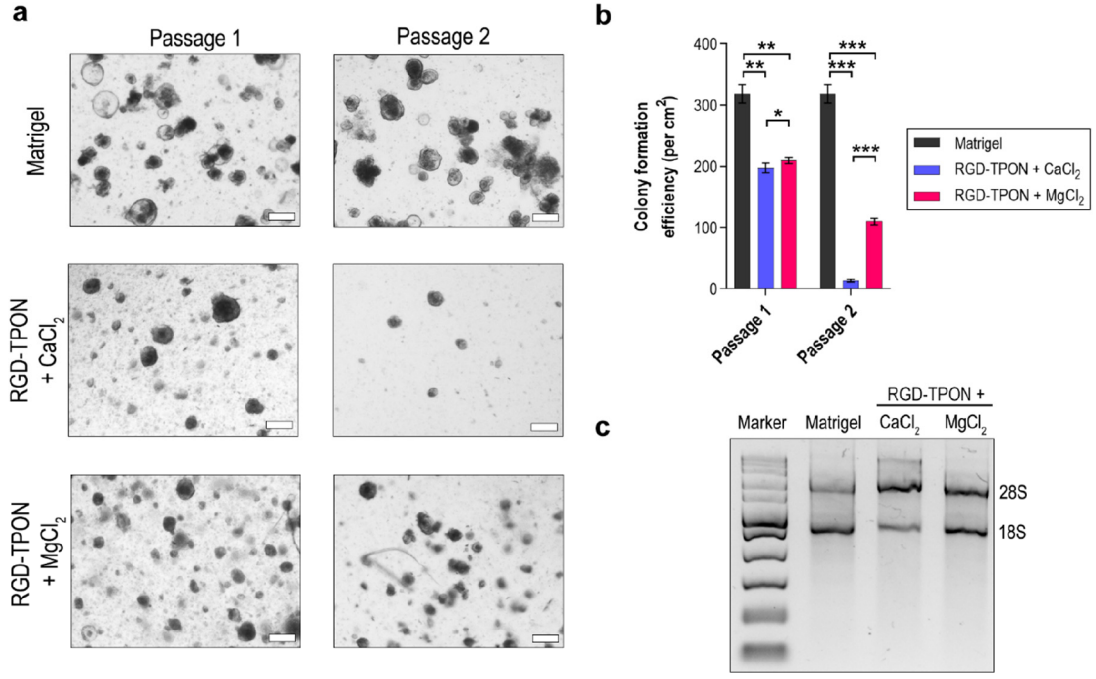

Figure 4. Intestinal organoids passage and recovery. (A) Intestinal organoids are easily passaged and grow in the magnesium-cross-linked matrix, while those in calcium-containing gels are in very low numbers. (B) Colony formation efficiency shows the number of organoids passaged in Mg gels to be 10 times higher than in calcium gels. (C) RNA extracted from nanocellulose matrix is intact. Scale bars: 200 μm. Results shown represent independent experiments performed in triplicates (n = 3, error bars = SD). *p < 0.05. **p < 0.005. ***p < 0.0005.

TON hydrogel remains mostly cystic (an irregular spherical morphology) with minor signals of budding, while organoids in RGD-TPON have more prominent buds (Figure 1g).

Rheological Analysis of Calcium- and Magnesium-Cross-Linked Hydrogels. The mechanical properties of RGD-TPON hydrogels cross-linked with $MgCl_2$ and $CaCl_2$ were characterized by rheology. The storage modulus (G') of RGD-TPON gels ranges from 75 to 150 Pa when cross-linked with 50 and 200 mM Ca^{2+} ions, respectively. (Figure 2a). In contrast, the stiffness (G') of magnesium-cross-linked gels varies from 20 to 66 Pa under the same concentrations of Mg^{2+} ions. The oscillatory strain sweep reveals hydrogels cross-linked with $MgCl_2$ (200 mM) and $CaCl_2$ (50 mM) to have a viscoelastic profile comparable to Matrigel (Figure 2b,c). The viscosity curves show all cellulose hydrogels as well as Matrigel to have a characteristic shear-thinning behavior (Figure 2d). Last, the yielding point of Matrigel is 48 Pa, while the cellulosic matrices flow under 6 and 9 Pa when cross-linked with magnesium and calcium, respectively (Figure 2e).

Intestinal Organoids Viability. To assess the cytotoxicity of the RGD-TPON hydrogels, intestinal organoids are encapsulated in the cellulosic matrixes and cultured for 4 days. On the second and fourth day, organoids are stained with Calcein-AM and propidium iodide to determine the living and dead area, respectively. On the second day of culture, organoids in Matrigel and RGD-TPON gels present a cystic morphology without any signals of cell death. On the fourth day, intestinal organoids embedded in calcium- and magnesium-cross-linked hydrogels show a small cluster of apoptotic cells while maintaining a major viable area. Similarly, organoids in Matrigel have minor loss of cells by apoptosis and preserve the epithelial integrity (Figure 3).

https://dx.doi.org/10.1021/acs.biomac.0c01510
Biomacromolecules 2021, 22, 701−709

Organoids Recovery for Passaging and RNA Extraction. On the fourth day of culture, the colony formation efficiencies of RGD-TPON hydrogels and Matrigel are quantified, and organoids were recovered (dislodged from the matrices) for RNA extraction. In spite of the ionic cross-linker used, RGD-TPON hydrogels can grow organoids at a quantity of nearly 200 organoids/cm^2. In Matrigel, the number of intestinal organoids reaches 300 units/cm^2, nearly 30% more than for the cellulosic matrices (Figure 4a). After passaging, a similar number of organoids can still grow in Matrigel. However, the number of organoids in calcium-cross-linked hydrogels sustains a massive decrease and reaches 10 organoids/cm^2. In contrast, RGD-TPON gels cross-linked with Mg^{2+} ions can grow organoids at 100 units/cm^2 (Figure 4b). The RNA of the intestinal organoids dislodged from RGD-TPON hydrogels and Matrigel was extracted and tested for integrity. Samples were run in an electrophoresis gel, and two characteristic bands are detected at 28S and 18S (Figure 4c). In addition, the RNA integrity number (RIN) for RNA samples collected from nanocellulose and Matrigel is scored between 7 and 9 (Figure S4). This reveals that the RNA of organoids cultured in all three matrices is intact and can be used for further biological analysis.

DISCUSSION

In this study, cationic cross-linked nanocellulose hydrogels are evaluated as matrices for the growth and recovery of intestinal organoids. Cellulose-based gels were previously explored as inert scaffolds for the tissue engineering and differentiation of cells.[16,34,37] These materials are limited by the absence of cell adhesive sites which do not recreate the biochemical conditions of animal tissues. In addition, the physical properties of neat cellulosic gels are dependent on its solids content, preventing the easy and fast recovery of organoids. Here, we demonstrate that oxidized nanocellulose fibers can be functionalized with cell adhesive sites and then cross-linked with Ca^{2+} and Mg^{2+} ions to grow and then recover intestinal organoids. First, TON and TPON gels were assessed for their abilities to support the culture of organoids. Because of their highly carboxylated cellulosic backbone, TPON fibers allow grafting of RGD peptides at higher levels than TON fibers. RGD peptides were covalently bound to the nanocellulose fibers by carbodiimide-induced cross-linking, in which the carboxylate groups are first activated by EDC and NHS in the absence of the peptides. Only in the second step, RGD peptides are added to the reaction to minimize its eventual aggregation due to interaction between its carboxyl and amine groups. The fibronectin-derived moieties are important to enhance the interaction between the cells and the cellulosic surface, hence mimicking the conditions found in the extracellular matrix (ECM). In general, the presence of these peptides regulates the cell proliferation and differentiation.[38,39] Successful biomaterials that support cell and organoid growth are reported to have integrin-binding ligands—such as RGD, IKVAV, and YIGSR peptides—at a concentration of 0.5−2 mM.[29,30] As important as the biological cues, the mechanical properties of the hydrogels must resemble the stiffness of organs and tissues.[26,40] By targeting the storage modulus (G') measured for Matrigel, RGD-TON and RGD-TPON hydrogels at 0.1 wt % were cross-linked with calcium ions. Because of the higher carboxyl content of TPON, the netpoint density of these hydrogels is 55% higher than in TON, even after grafted with RGD. Hence, the RGD-TPON hydrogels form a stiffer 3D network compared to RGD-TON and closer to that of Matrigel. Organoids cultured in these RGD-TPON hydrogels present a mature morphology characterized by the presence of prominent budding structures. In contrast, organoids embedded in RGD-TON gels remain mostly cystic with only minor signals of development. These results suggest the RGD-TPON hydrogels to offer an optimum bioactive surface and appropriate stiffness for organoid attachment and growth. Interestingly, the optical properties of RGD-TPON hydrogels are not affected by grafting peptides on the cellulose backbone. TPON hydrogels are highly transparent materials with optical properties superior to those of TON hydrogels and Matrigel.[13] By allowing nearly 100% of light to be transmitted, RGD-TPON hydrogels support the advanced imaging of intracellular structures, like organelles and proteins, usually achieved by confocal microscopy.

The 3D network of hydrogels relies on the cross-linking of the polymer chains to form a continuous fibrous and porous structure.[41,42] The cross-link between polymeric units can be achieved by chemical or physical interactions.[43] Chemically cross-linked hydrogels generally present robust and stable covalent bonds, and the effective cleavage of these bonds may require enzymes or radiation to occur.[44−46] By contrast, physical cross-linking is coordinated by reversible associations between the electronegative functional groups present in the polymer chains.[10,47] The addition of ions to connect the polymeric chains increases the mechanical properties of the hydrogels, while this binding can easily be disrupted by shear forces.[48−50] Although calcium chloride is a classic ionic cross-linking agent of hydrogels, its excess can be hazardous to cell cultures. Indeed, many studies reported that Ca^{2+} ions in nonphysiological levels can induce apoptosis of different cell types.[51−53] In addition, nanocellulose hydrogels cross-linked with Ca^{2+} were recently reported to induce the overexpression of calcium-dependent genes in intestinal organoids.[35] In contrast, magnesium-cross-linked materials have not been investigated in depth as a cross-linker for biomaterials for 3D cell culture nor in regards to their eventual effects over multicellular clusters such as organoids.[54] To the best of our knowledge, the excess of Mg^{2+} ions have only been assessed as an apoptotic agent in prostate cancer cell lines and also to reduce excitability of neurons.[55,56] In this context, we compared the cross-linking of nanocellulose matrices with both ionic agents. Starting from a material's perspective, we investigate the equivalent concentration of magnesium chloride required for RGD-TPON to achieve the mechanical properties of Matrigel. Donati et al. reported Mg^{2+} ions and alginate fibers to present a weaker interaction than Ca^{2+} ions.[57] While calcium ions strongly bind to a specific site, magnesium ions are described as a "diffusively bound counterion", which translates in materials of lower mechanical properties.[58,59] Indeed, we reveal that RGD-TPON hydrogels require 4 times more Mg^{2+} ions to achieve the same stiffness as those hydrogels cross-linked with calcium. Although the oscillatory strain sweep and viscosity measurements present similar curves, the yielding point of magnesium-cross-linked gels (200 mM) is 33% lower than for calcium-containing gels (50 mM). This highlights the fragility of the bonds between magnesium and carboxylate nanocellulose and presents two direct benefits. First, the 3D structure of the hydrogel can be remodeled by the organoids while their cells are growing and proliferating. Indeed, the entangled network of the hydrogels can self-heal in response to mechanical stimulus to rearrange

https://dx.doi.org/10.1021/acs.biomac.0c01510
Biomacromolecules 2021, 22, 701−709

its internal 3D structure while the cells progress into complex self-organized systems like organoids.[60−62] Second, the matrix can be completely disrupted by manual pipetting to separate the organoids from the hydrogel. Both processes do not require the use of enzymes to digest the cellulose nanofibers, supporting not only the proper development of the organoids but also their efficient recovery.

Last, calcium- and magnesium-cross-linked RGD-TPON hydrogels are compared for their abilities to grow intestinal organoids and the recovery of these clusters of cells. Although cross-linked hydrogels are shown to be noncytotoxic, the colony formation efficiency in both matrices is nearly 30% lower than in Matrigel in the first passage. On the second passage, the number of organoids formed in magnesium-cross-linked RGD-TPON gels reduces to 50%, while in hydrogels cross-linked with calcium this reduction is nearly 95%. This suggests that calcium ions may compromise the self-renewability of intestinal organoids by affecting the stem cell population that sustains organoids for long-term culture. In contrast, the efficiency of the magnesium-cross-linked matrix remains considerably higher with the growth rate measured comparable to recent studies.[33,63] Synthetic matrices are naturally less efficient than Matrigel due to the absence of several growth factors responsible to enhance the proliferation and differentiation of cells. In addition, Matrigel is made of multiple fibrous proteins—including laminin, collagen, and entactin—that contain many integrin-binding sites inducing cell growth.[27,28,64] TPON hydrogels are functionalized with a single cell adhesive site, RGD, which accounts for its lower performance. In spite of this differences, organoids can be easily recovered from RGD-TPON hydrogels for biological characterization. The RNA extracted from organoids cultured in the hydrogels remains intact and allow further analysis such as the whole transcriptome sequencing. To perform this assay, not only the cells need to be recovered but also their RNA must be preserved for reliable tests. As an example, the quantification of the genes expressed by organoids grown in nanocellulose may reveal the biochemical pathways up and downregulated by the matrix. Based on this information, the lacking additives—such as proteins and growth factors—can then be properly identified and targeted. Overall, magnesium-cross-linked TPON hydrogels represent a new class of promising materials for the short-term culture of intestinal organoids.

CONCLUSION

Cellulose-based hydrogels are plant-based sustainable and low-cost soft materials with strong potential for applications in biomedicine. Such alternative materials are urgently needed for 3D cell culture to reduce the dependency of the standard animal-based tumor-derived gels currently used. In this study, we demonstrate that cationic cross-linked nanocellulose hydrogels can efficiently grow intestinal organoids. Because of its higher carboxyl content, TPON fibers allow the grafting of more RGD peptides than TON, providing the desired biochemical cues for cell adhesion. RGD-TPON can be engineered to achieve the required mechanical properties by using magnesium and calcium ions as cationic cross-linkers. Interestingly, magnesium-cross-linked hydrogels sustain the culture of organoids that can be passaged, with their RNA extracted remaining intact, enabling further biological analysis. In contrast, calcium-containing gels are limited by critically reducing the number of organoids grown after multiple passages. In this study, murine intestinal organoids were adopted as biological models. The suitability of these hydrogels for other types of organoids, including those derived from human tissues, remains to be individually assessed. Moreover, additives like extracellular matrix factors and proteins, such as collagens and laminin, could be blended to the hydrogel to provide the biological microenvironment required for specific cell types. Cationic cross-linked nanocellulose matrices stand as a promising and performant material for the 3D cell culture systems, with potential to reduce costs in biomedical research.

ASSOCIATED CONTENT

Supporting Information

The Supporting Information is available free of charge at https://pubs.acs.org/doi/10.1021/acs.biomac.0c01510.

Figures S1−S4 and Table S1 (PDF)

AUTHOR INFORMATION

Corresponding Author

Gil Garnier − *Bioresource Processing Research Institute of Australia (BioPRIA), Department of Chemical Engineering, Monash University, Melbourne, Australia;* orcid.org/0000-0003-3512-0056; Email: gil.garnier@monash.edu

Author

Rodrigo Curvello − *Bioresource Processing Research Institute of Australia (BioPRIA), Department of Chemical Engineering, Monash University, Melbourne, Australia*

Complete contact information is available at: https://pubs.acs.org/10.1021/acs.biomac.0c01510

Author Contributions

R.C. designed and performed all the experiments and wrote the manuscript. G.G. reviewed the manuscript and provided scientific vision and consultation along the study.

Notes

The authors declare no competing financial interest.

ACKNOWLEDGMENTS

This work was funded by the Australian Research Council-Industry Transformation Research Hub; Processing Advanced Lignocellulosics (PALS) IH170100020 and ARC LP160100544. Many thanks to the Australian Paper, Maryvale, Australia, for providing the pulp. The authors acknowledge the resources, facility, and staff of the Biomedicine Discovery Institute Organoid Program at Monash University, Victoria, Australia. Thanks to Dr. Diana J. Micati for kindly helping with the RNA extraction, Professor Rico F. Tabor for discussions, Diana Alves and David Mendoza for experimental design and discussion, and Virginia A. Garnier for helping with the culture of organoids.

REFERENCES

(1) Mitrousis, N.; Fokina, A.; Shoichet, M. S. Biomaterials for cell transplantation. *Nat. Rev. Mater.* **2018**, *3* (11), 441−456.

(2) Prince, E.; Kumacheva, E. Design and applications of man-made biomimetic fibrillar hydrogels. *Nat. Rev. Mater.* **2019**, *4* (2), 99−115.

(3) Klouda, L.; Mikos, A. G. Thermoresponsive hydrogels in biomedical applications. *Eur. J. Pharm. Biopharm.* **2008**, *68* (1), 34−45.

(4) Krogsgaard, M.; Behrens, M. A.; Pedersen, J. S.; Birkedal, H. Self-Healing Mussel-Inspired Multi-pH-Responsive Hydrogels. *Biomacromolecules* **2013**, *14* (2), 297−301.

(5) Tomatsu, I.; Peng, K.; Kros, A. Photoresponsive hydrogels for biomedical applications. *Adv. Drug Delivery Rev.* **2011**, *63* (14), 1257−1266.
(6) Capeling, M. M.; Czerwinski, M.; Huang, S.; Tsai, Y.-H.; Wu, A.; Nagy, M. S.; Juliar, B.; Sundaram, N.; Song, Y.; Han, W. M.; Takayama, S.; Alsberg, E.; Garcia, A. J.; Helmrath, M.; Putnam, A. J.; Spence, J. R. Nonadhesive Alginate Hydrogels Support Growth of Pluripotent Stem Cell-Derived Intestinal Organoids. *Stem Cell Rep.* **2019**, *12* (2), 381−394.
(7) Bhattarai, N.; Gunn, J.; Zhang, M. Chitosan-based hydrogels for controlled, localized drug delivery. *Adv. Drug Delivery Rev.* **2010**, *62* (1), 83−99.
(8) Du, H.; Liu, W.; Zhang, M.; Si, C.; Zhang, X.; Li, B. Cellulose nanocrystals and cellulose nanofibrils based hydrogels for biomedical applications. *Carbohydr. Polym.* **2019**, *209*, 130−144.
(9) Salas, C.; Nypelö, T.; Rodriguez-Abreu, C.; Carrillo, C.; Rojas, O. J. Nanocellulose properties and applications in colloids and interfaces. *Curr. Opin. Colloid Interface Sci.* **2014**, *19* (5), 383−396.
(10) Curvello, R.; Raghuwanshi, V. S.; Garnier, G. Engineering nanocellulose hydrogels for biomedical applications. *Adv. Colloid Interface Sci.* **2019**, *267*, 47−61.
(11) Saito, T.; Kimura, S.; Nishiyama, Y.; Isogai, A. Cellulose Nanofibers Prepared by TEMPO-Mediated Oxidation of Native Cellulose. *Biomacromolecules* **2007**, *8* (8), 2485−2491.
(12) Mendoza, D. J.; Browne, C.; Raghuwanshi, V. S.; Simon, G. P.; Garnier, G. One-shot TEMPO-periodate oxidation of native cellulose. *Carbohydr. Polym.* **2019**, *226*, 115292.
(13) Mendoza, D. J.; Hossain, L.; Browne, C.; Raghuwanshi, V. S.; Simon, G. P.; Garnier, G. Controlling the transparency and rheology of nanocellulose gels with the extent of carboxylation. *Carbohydr. Polym.* **2020**, *245*, 116566.
(14) Mendoza, L.; Batchelor, W.; Tabor, R. F.; Garnier, G. Gelation mechanism of cellulose nanofibre gels: A colloids and interfacial perspective. *J. Colloid Interface Sci.* **2018**, *509*, 39−46.
(15) Curvello, R.; Mendoza, L.; McLiesh, H.; Manolios, J.; Tabor, R. F.; Garnier, G. Nanocellulose Hydrogel for Blood Typing Tests. *ACS Applied Bio Materials* **2019**, *2* (6), 2355−2364.
(16) Bhattacharya, M.; Malinen, M. M.; Lauren, P.; Lou, Y.-R.; Kuisma, S. W.; Kanninen, L.; Lille, M.; Corlu, A.; GuGuen-Guillouzo, C.; Ikkala, O.; Laukkanen, A.; Urtti, A.; Yliperttula, M. Nanofibrillar cellulose hydrogel promotes three-dimensional liver cell culture. *J. Controlled Release* **2012**, *164* (3), 291−298.
(17) Azoidis, I.; Metcalfe, J.; Reynolds, J.; Keeton, S.; Hakki, S. S.; Sheard, J.; Widera, D. Three-dimensional cell culture of human mesenchymal stem cells in nanofibrillar cellulose hydrogels. *MRS Commun.* **2017**, *7* (3), 458−465.
(18) Mohd Amin, M. C. I.; Ahmad, N.; Halib, N.; Ahmad, I. Synthesis and characterization of thermo- and pH-responsive bacterial cellulose/acrylic acid hydrogels for drug delivery. *Carbohydr. Polym.* **2012**, *88* (2), 465−473.
(19) Jack, A. A.; Nordli, H. R.; Powell, L. C.; Powell, K. A.; Kishnani, H.; Johnsen, P. O.; Pukstad, B.; Thomas, D. W.; Chinga-Carrasco, G.; Hill, K. E. The interaction of wood nanocellulose dressings and the wound pathogen P. aeruginosa. *Carbohydr. Polym.* **2017**, *157*, 1955−1962.
(20) Shamir, E. R.; Ewald, A. J. Three-dimensional organotypic culture: experimental models of mammalian biology and disease. *Nat. Rev. Mol. Cell Biol.* **2014**, *15* (10), 647−664.
(21) Qiao, H.; Tang, T. Engineering 3D approaches to model the dynamic microenvironments of cancer bone metastasis. *Bone Res.* **2018**, *6* (1), 3.
(22) Liu, Z.; Tang, M.; Zhao, J.; Chai, R.; Kang, J. Looking into the Future: Toward Advanced 3D Biomaterials for Stem-Cell-Based Regenerative Medicine. *Adv. Mater.* **2018**, *30* (17), 1705388.
(23) Clevers, H. Modeling Development and Disease with Organoids. *Cell* **2016**, *165* (7), 1586−1597.
(24) Rossi, G.; Manfrin, A.; Lutolf, M. P. Progress and potential in organoid research. *Nat. Rev. Genet.* **2018**, *19* (11), 671−687.
(25) van de Wetering, M.; Francies, H. E.; Francis, J. M.; Bounova, G.; Iorio, F.; Pronk, A.; van Houdt, W.; van Gorp, J.; Taylor-Weiner, A.; Kester, L.; McLaren-Douglas, A.; Blokker, J.; Jaksani, S.; Bartfeld, S.; Volckman, R.; van Sluis, P.; Li, V. S. W.; Seepo, S.; Sekhar Pedamallu, C.; Cibulskis, K.; Carter, S. L.; McKenna, A.; Lawrence, M. S.; Lichtenstein, L.; Stewart, C.; Koster, J.; Versteeg, R.; van Oudenaarden, A.; Saez-Rodriguez, J.; Vries, R. G. J.; Getz, G.; Wessels, L.; Stratton, M. R.; McDermott, U.; Meyerson, M.; Garnett, M. J.; Clevers, H. Prospective Derivation of a Living Organoid Biobank of Colorectal Cancer Patients. *Cell* **2015**, *161* (4), 933−945.
(26) Kratochvil, M. J.; Seymour, A. J.; Li, T. L.; Paşca, S. P.; Kuo, C. J.; Heilshorn, S. C. Engineered materials for organoid systems. *Nat. Rev. Mater.* **2019**, *4* (9), 606−622.
(27) Hughes, C. S.; Postovit, L. M.; Lajoie, G. A. Matrigel: A complex protein mixture required for optimal growth of cell culture. *Proteomics* **2010**, *10* (9), 1886−1890.
(28) Aisenbrey, E. A.; Murphy, W. L. Synthetic alternatives to Matrigel. *Nat. Rev. Mater.* **2020**, *5*, 539.
(29) Cruz-Acuña, R.; Quirós, M.; Farkas, A. E.; Dedhia, P. H.; Huang, S.; Siuda, D.; García-Hernández, V.; Miller, A. J.; Spence, J. R.; Nusrat, A.; García, A. J. Synthetic hydrogels for human intestinal organoid generation and colonic wound repair. *Nat. Cell Biol.* **2017**, *19* (11), 1326−1335.
(30) Gjorevski, N.; Sachs, N.; Manfrin, A.; Giger, S.; Bragina, M. E.; Ordóñez-Morán, P.; Clevers, H.; Lutolf, M. P. Designer matrices for intestinal stem cell and organoid culture. *Nature* **2016**, *539* (7630), 560−564.
(31) Broguiere, N.; Isenmann, L.; Hirt, C.; Ringel, T.; Placzek, S.; Cavalli, E.; Ringnalda, F.; Villiger, L.; Züllig, R.; Lehmann, R.; Rogler, G.; Heim, M. H.; Schüler, J.; Zenobi-Wong, M.; Schwank, G. Growth of Epithelial Organoids in a Defined Hydrogel. *Adv. Mater.* **2018**, *30* (43), 1801621.
(32) Ye, S.; Boeter, J. W.B.; Mihajlovic, M.; Steenbeek, F. G.; Wolferen, M. E.; Oosterhoff, L. A.; Marsee, A.; Caiazzo, M.; Laan, L. J. W.; Penning, L. C.; Vermonden, T.; Spee, B.; Schneeberger, K. A Chemically Defined Hydrogel for Human Liver Organoid Culture. *Adv. Funct. Mater.* **2020**, *30*, 2000893.
(33) Yavitt, F. M.; Brown, T. E.; Hushka, E. A.; Brown, M. E.; Gjorevski, N.; Dempsey, P. J.; Lutolf, M. P.; Anseth, K. S. The Effect of Thiol Structure on Allyl Sulfide Photodegradable Hydrogels and their Application as a Degradable Scaffold for Organoid Passaging. *Adv. Mater.* **2020**, *32* (30), 1905366.
(34) Krüger, M.; Oosterhoff, L. A.; van Wolferen, M. E.; Schiele, S. A.; Walther, A.; Geijsen, N.; De Laporte, L.; van der Laan, L. J. W.; Kock, L. M.; Spee, B. Cellulose Nanofibril Hydrogel Promotes Hepatic Differentiation of Human Liver Organoids. *Adv. Healthcare Mater.* **2020**, *9* (6), 1901658.
(35) Curvello, R.; Kerr, G.; Micati, D. J.; Chan, W. H.; Raghuwanshi, V. S.; Rosenbluh, J.; Abud, H. E.; Garnier, G. Engineered Plant-Based Nanocellulose Hydrogel for Small Intestinal Organoid Growth. *Adv. Sci.* **2020**, 2002135.
(36) Flory, P. J.; Rehner, J. Statistical Mechanics of Cross-Linked Polymer Networks II. Swelling. *J. Chem. Phys.* **1943**, *11* (11), 521−526.
(37) Markstedt, K.; Mantas, A.; Tournier, I.; Martínez Ávila, H.; Hägg, D.; Gatenholm, P. 3D Bioprinting Human Chondrocytes with Nanocellulose−Alginate Bioink for Cartilage Tissue Engineering Applications. *Biomacromolecules* **2015**, *16* (5), 1489−1496.
(38) Kechagia, J. Z.; Ivaska, J.; Roca-Cusachs, P. Integrins as biomechanical sensors of the microenvironment. *Nat. Rev. Mol. Cell Biol.* **2019**, *20* (8), 457−473.
(39) Shattil, S. J.; Kim, C.; Ginsberg, M. H. The final steps of integrin activation: the end game. *Nat. Rev. Mol. Cell Biol.* **2010**, *11* (4), 288−300.
(40) Guimarães, C. F.; Gasperini, L.; Marques, A. P.; Reis, R. L. The stiffness of living tissues and its implications for tissue engineering. *Nat. Rev. Mater.* **2020**, *5* (5), 351−370.
(41) Paterson, S. M.; Clark, J.; Stubbs, K. A.; Chirila, T. V.; Baker, M. V. Carbohydrate-based crosslinking agents: Potential use in

hydrogels. *J. Polym. Sci., Part A: Polym. Chem.* **2011**, *49* (20), 4312−4315.
(42) Hennink, W. E.; van Nostrum, C. F. Novel crosslinking methods to design hydrogels. *Adv. Drug Delivery Rev.* **2012**, *64*, 223−236.
(43) Hu, W.; Wang, Z.; Xiao, Y.; Zhang, S.; Wang, J. Advances in crosslinking strategies of biomedical hydrogels. *Biomater. Sci.* **2019**, *7* (3), 843−855.
(44) Nezhad-Mokhtari, P.; Ghorbani, M.; Roshangar, L.; Soleimani Rad, J. Chemical gelling of hydrogels-based biological macromolecules for tissue engineering: Photo- and enzymatic-crosslinking methods. *Int. J. Biol. Macromol.* **2019**, *139*, 760−772.
(45) Hushka, E. A.; Yavitt, F. M.; Brown, T. E.; Dempsey, P. J.; Anseth, K. S. Relaxation of Extracellular Matrix Forces Directs Crypt Formation and Architecture in Intestinal Organoids. *Adv. Healthcare Mater.* **2020**, *9* (8), 1901214.
(46) Hong, L. T. A.; Kim, Y.-M.; Park, H. H.; Hwang, D. H.; Cui, Y.; Lee, E. M.; Yahn, S.; Lee, J. K.; Song, S.-C.; Kim, B. G. An injectable hydrogel enhances tissue repair after spinal cord injury by promoting extracellular matrix remodeling. *Nat. Commun.* **2017**, *8* (1), 533.
(47) de Gennes, P. G. Polymer gels. In *Scaling Concepts in Polymer Physics*; Cornell University Press: 1979; pp 128−38.
(48) Berger, J.; Reist, M.; Mayer, J. M.; Felt, O.; Peppas, N. A.; Gurny, R. Structure and interactions in covalently and ionically crosslinked chitosan hydrogels for biomedical applications. *Eur. J. Pharm. Biopharm.* **2004**, *57* (1), 19−34.
(49) Moura, M. J.; Faneca, H.; Lima, M. P.; Gil, M. H.; Figueiredo, M. M. In Situ Forming Chitosan Hydrogels Prepared via Ionic/Covalent Co-Cross-Linking. *Biomacromolecules* **2011**, *12* (9), 3275−3284.
(50) Rouillard, A. D.; Tsui, Y.; Polacheck, W. J.; Lee, J. Y.; Bonassar, L. J.; Kirby, B. J. Control of the Electromechanical Properties of Alginate Hydrogels via Ionic and Covalent Cross-Linking and Microparticle Doping. *Biomacromolecules* **2010**, *11* (8), 2184−2189.
(51) Orrenius, S.; Zhivotovsky, B.; Nicotera, P. Regulation of cell death: the calcium−apoptosis link. *Nat. Rev. Mol. Cell Biol.* **2003**, *4* (7), 552−565.
(52) Schanne, F. A.; Kane, A. B.; Young, E. E.; Farber, J. L. Calcium dependence of toxic cell death: a final common pathway. *Science* **1979**, *206* (4419), 700.
(53) Wertz, I. E.; Dixit, V. M. Characterization of Calcium Release-activated Apoptosis of LNCaP Prostate Cancer Cells. *J. Biol. Chem.* **2000**, *275* (15), 11470−11477.
(54) Ishaque, A.; Al-Rubeai, M. Role of Ca2+, Mg2+ and K+ ions in determining apoptosis and extent of suppression afforded by bcl-2 during hybridoma cell culture. *Apoptosis* **1999**, *4* (5), 335−355.
(55) Dribben, W. H.; Eisenman, L. N.; Mennerick, S. Magnesium induces neuronal apoptosis by suppressing excitability. *Cell Death Dis.* **2010**, *1* (8), e63−e63.
(56) Santos, J.; Hussain, F. Magnesium Chloride increases apoptosis and decreases prostate cancer cells migration. *Funct. Foods Health Dis.* **2018**, *8*, 62−78.
(57) Donati, I.; Asaro, F.; Paoletti, S. Experimental Evidence of Counterion Affinity in Alginates: The Case of Nongelling Ion Mg2+. *J. Phys. Chem. B* **2009**, *113* (39), 12877−12886.
(58) Topuz, F.; Henke, A.; Richtering, W.; Groll, J. Magnesium ions and alginate do form hydrogels: a rheological study. *Soft Matter* **2012**, *8* (18), 4877−4881.
(59) Donati, I.; Cesàro, A.; Paoletti, S. Specific Interactions versus Counterion Condensation. 1. Nongelling Ions/Polyuronate Systems. *Biomacromolecules* **2006**, *7* (1), 281−287.
(60) Talebian, S.; Mehrali, M.; Taebnia, N.; Pennisi, C. P.; Kadumudi, F. B.; Foroughi, J.; Hasany, M.; Nikkhah, M.; Akbari, M.; Orive, G.; Dolatshahi-Pirouz, A. Self-Healing Hydrogels: The Next Paradigm Shift in Tissue Engineering? *Advanced Science* **2019**, *6* (16), 1801664.
(61) Liu, Y.; Hsu, S.-h. Synthesis and Biomedical Applications of Self-healing Hydrogels. *Front. Chem.* **2018**, *6*, 449.
(62) Deng, Z.; Wang, H.; Ma, P. X.; Guo, B. Self-healing conductive hydrogels: preparation, properties and applications. *Nanoscale* **2020**, *12* (3), 1224−1246.
(63) Rezakhani, S.; Gjorevski, N.; Lutolf, M. P. Low-Defect Thiol-Michael Addition Hydrogels as Matrigel Substitutes for Epithelial Organoid Derivation. *Adv. Funct. Mater.* **2020**, *30*, 2000761.
(64) Kleinman, H. K.; Martin, G. R. Matrigel: Basement membrane matrix with biological activity. *Semin. Cancer Biol.* **2005**, *15* (5), 378−386.

https://dx.doi.org/10.1021/acs.biomac.0c01510
Biomacromolecules 2021, 22, 701−709